Optical Materials 35 (2013) 2486–2489

Contents lists available at ScienceDirect

Optical Materials

journal homepage: www.elsevier.com/locate/optmat

Effect of compressive stress on doping efficiency of nitrogen in ZnO films

Wei-Wei Liu [a], Zhen-Zhong Zhang [b,*], Bin Yao [c,*], De-Zhen Shen [b], Cheng-Lin Liu [a]

[a] Department of Physics Science & Technology, Yancheng Teachers University, Yancheng 224002, China
[b] State Key Laboratory of Luminescence and Applications, Changchun Institute of Optics, Fine Mechanics and Physics, Chinese Academy of Sciences, No.3888 Dongnanhu Road, Changchun 130021, China
[c] Department of Physics, Jilin University, Changchun 130023, China

ARTICLE INFO

Article history:
Received 2 April 2013
Received in revised form 30 June 2013
Accepted 1 July 2013
Available online 13 August 2013

Keywords:
ZnO
Stress
Doping efficiency
N-doped

ABSTRACT

Nitrogen (N)-doped ZnO films (ZnO:N) grown on the *a*-/*c*-plane sapphire substrates (*a*-/*c*-Al_2O_3) by plasma-assisted molecular beam epitaxy were investigated. It was found that the content of N in the ZnO films grown on *c*-Al_2O_3 is higher than that of the films grown on *a*-Al_2O_3. The ZnO:N films grown on *c*-Al_2O_3 have lower carrier concentration and larger intensity ratio of the DAP/D°X emission compared with those of the ZnO:N films grown on *a*-Al_2O_3 under the same growth conditions, which indicates higher incorporation efficiency of N in the ZnO films grown on *c*-Al_2O_3.

1. Introduction

Zinc oxide (ZnO) was considered as a promising material for optical device application in the blue and ultraviolet wavelength region owing to its direct wide band gap ($E_g \sim 3.3$ eV at 300 K) and large exciton binding energy (60 meV) [1,2]. However, it has been proved to be very difficult to produce a stable *p*-type ZnO with high conductivity and mobility. Many factors affect the quality of *p*-type films, such as growth temperature, dopants and substrate, etc. Since growth temperature affects the solubility limit of dopants, suitable growth temperature should be determined to obtain high incorporation efficiency of dopants [3]. Recently, many research groups have reported the *p*-type ZnO by single doping of I or V group elements, such as N, P, Li, and [4–6], and codoping of III–V groups, such as Ga–P, Al–N, Li–N, Ga–N, etc [7–10]. Among these dopants, N is thought to be the best candidate for producing a shallow *p*-type dopant in ZnO, because it has the closest atomic size and electronic structure to oxygen. Some groups are also reported that they obtained *p*-type ZnO films using different substrates, such as Al_2O_3 (0001), Si (100), bulk ZnO, glass, and $ScAlMgO_4$ (0001), [11–16]. From their reports, it can be found that the properties of the films can be greatly modulated by varying substrates. However, systematic investigation on the relationship between N incorporation efficiency and substrate is rare. So in this paper we report our study of the effect of stress caused by lattice mismatch between ZnO films and *a*-/*c*-plane sapphire substrates (*a*-/*c*-Al_2O_3) on the doping efficiency of nitrogen in the ZnO films. For convenience, ZnO:N films grown on *a*-Al_2O_3 and *c*-Al_2O_3 were denoted by ZnO:N⟨*a*⟩ and ZnO:N⟨*c*⟩, respectively.

2. Experiments

ZnO:N films were grown by plasma-assisted molecular beam epitaxy on *a*-/*c*-Al_2O_3 at 450 °C, respectively. The substrates surface was pre-exposure in O-plasma at 500 °C for 10 min before growth. NO gas (99.99%) was used as O source and N dopant and activated during the growth process by an Oxford Applied Research Model HD25 rf (13.56 MHz) atomic source. The NO flux was fixed at 0.8 SCCM (SCCM denotes cubic centimeter per minute at standard temperature and pressure). The Zn source temperature (T_{Zn}) was changed from 235 to 255 °C with steps of 5 °C. The thicknesses of the films increased from 465 to 700 nm and from 500 to 745 nm for ZnO:N films grown on *a*- and *c*-Al_2O_3, respectively, while the Zn cell temperatures increased from 235 °C to 255 °C. Structures of the films were characterized by a D/max-RA X-ray diffractometer (XRD) (Rigaku International Corp., Japan) with Cu Kα radiation. For the Raman scattering spectrum, polarized light from the 488 nm line of an Ar^+ ion laser was focused on the samples at room temperature. The scattered signal was dispersed by a Jobin–Yvon U1000 micro Raman spectrum using backscattering geometry. Electrical properties were measured in the van der Pauw configuration by a Hall-effect measurement system at room temperature. The low temperature photoluminescence (PL) measurement was

* Corresponding authors. Address: No. 50, Xiwang Road, Yancheng 130033, China.
E-mail addresses: exciton@163.com (Z.-Z. Zhang), yaobin196226@yahoo.com.cn (B. Yao).

0925-3467/$ - see front matter © 2013 Elsevier B.V. All rights reserved.
http://dx.doi.org/10.1016/j.optmat.2013.07.003

performed by the excitation from a 325 nm He–Cd laser with 50 mW power. X-ray photoelectron spectroscopy (XPS) measurement were performed by an ESCALAB 250 XPS instrument with Al Kα ($h\nu$ = 1486.6 eV) X-ray radiation source.

3. Results and discussion

ZnO has a hexagonal wurtzite structure and belongs to the C_6 symmetry group. The following Raman-active phonons were predicted for the wurtzite structure: an A_1 branch in which the phonon is polarized in the z direction; an E_1 branch in which the phonon is polarized in the xy plane, and two E_2 branches (the c axis of the crystal is taken to be the z axis). The E_1 branch is linearly polarized, but the two E_2 branches do not have a simple polarization behavior. A_1 and E_1 branches are polar with different energies for the longitudinal (LO) and transverse (TO) components. In the backscattering geometry, with the c axis normal to the surface, the TO branch of the A_1 mode and the TO and LO branches of the E_1 mode are forbidden. The LO branch of the E_2 modes (440 cm^{-1}) and A_1 mode (577 cm^{-1}) are allowed [17].

Raman scattering is performed on all of the samples at room temperature in back-scattering configuration. Undoped ZnO films grown on a-/c-Al_2O_3, ZnO:N⟨a⟩ films and ZnO:N⟨c⟩ films grown at the T_{Zn} of 235 °C, 250 °C and 255 °C were shown in Fig. 1a–d, respectively. The features marked by the asterisk are originated from a-/c-Al_2O_3. Besides the Raman peaks from sapphire substrates, a strong additional peak at 275 cm^{-1} appears in both ZnO:N⟨a⟩ and ZnO:N⟨c⟩ films, but not appears in the undoped ZnO films grown on a-/c-Al_2O_3, as shown in Fig. 1a–d, indicating that the Raman peak located at 275 cm^{-1} was related to N doping. Recently, Kaschner et al. found that the content of incorporated N in ZnO films can be quantitatively measured by Raman spectroscopy [18]. The stronger the peak located at 275 cm^{-1}, the larger N content in ZnO films. In our experiment, the intensity of 275 cm^{-1} Raman peaks increases with increasing T_{Zn}, indicating that the content of N in ZnO films increases with increasing T_{Zn} which is consistent with previous report [18]. Compared with ZnO:N⟨a⟩ films, the intensity of the peaks located at 275 cm^{-1} are always stronger for the ZnO:N⟨c⟩ films under the same growth conditions. This indicates that the ZnO:N⟨c⟩ films have larger N content at the same growth conditions. From XPS measurements, we found that, at the same T_{Zn}, the N_O content in the ZnO:N⟨c⟩ films (0.41% at T_{Zn} = 235 °C and 3.31% at T_{Zn} = 255 °C) is larger than that in the ZnO:N⟨a⟩ films (0.32% at T_{Zn} = 235 °C and 2.06% at T_{Zn} = 255 °C). Therefore, it can be concluded that N-doping with c-Al_2O_3 substrate has higher incorporation efficiency than with a-Al_2O_3 substrate.

The results of Hall-effect measurements for the ZnO:N⟨a⟩ and ZnO:N⟨c⟩ films grown at various T_{Zn} are summarized in Table 1a and b, respectively. The results show that the carrier concentration in both the ZnO:N⟨a⟩ and ZnO:N⟨c⟩ films increase first, and then decrease with increase of T_{Zn}. The increase in carrier concentration was attributed to the lower Zn beam flux while T_{Zn} lower than 245 °C. Further increase of T_{Zn} raises the Zn beam flux to a higher level. Under this condition, the formation energy of N_O was very low and the solubility of N was enhanced [19]. Numbers of oxygen vacancy (Vo) act as donor will be created under Zn-rich conditions, however, these donors were compensated by N_O acceptor which leads to high resistivity and low carrier concentration. From Table 1a and b, it can be found that the carrier concentration of the ZnO:N⟨c⟩ films is always lower than that of the ZnO:N⟨a⟩ films grown under the same growth conditions. A p-type ZnO:N film with hole concentration of 2.21 × 10^{16} cm^{-3} was obtained for the ZnO:N⟨c⟩ grown at the T_{Zn} of 255 °C. This means that the N_O has higher incorporation efficiency in ZnO:N⟨c⟩ films, which was consistent with Raman measurements. Above p-type ZnO films can be reproduced, however, the p-type conduction reverts to n-type conduction in a period of several days. Therefore, in order to obtain ultraviolet light-emitting diodes and lasers based on ZnO films, further investigation will be needed on the stability of p-type ZnO.

The epitaxial relationships between ZnO and c-Al_2O_3 can be seen elsewhere and the lattice mismatch was calculated to be

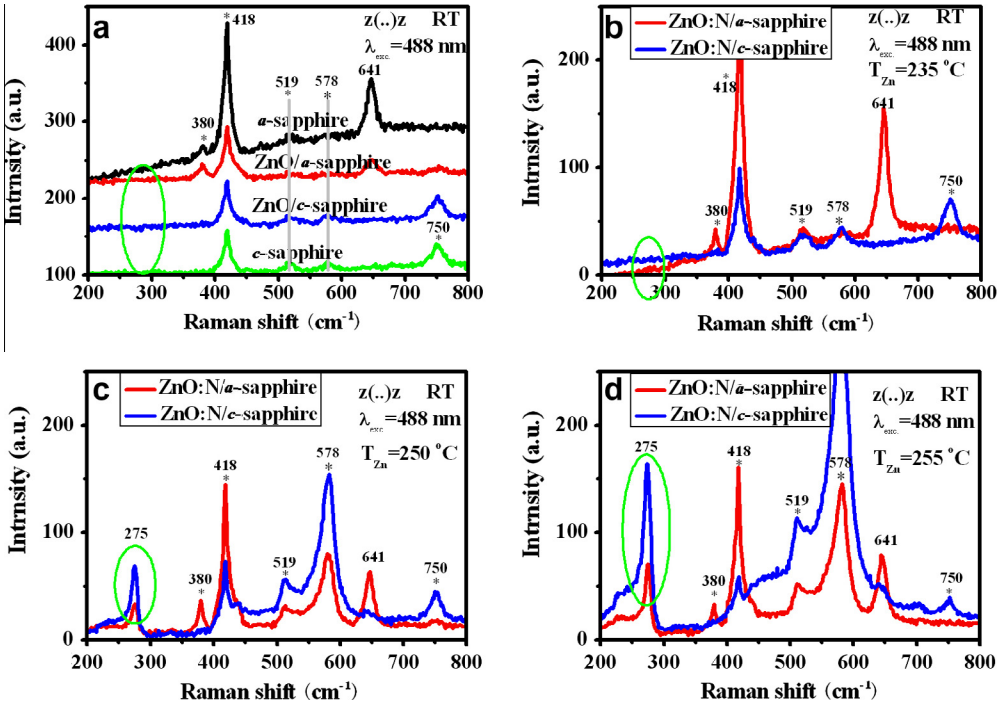

Fig. 1. Raman spectra from undoped ZnO films grown on a-/c-Al_2O_3 (a) ZnO:N films grown on a-/c-Al_2O_3 at the T_{Zn} of (b) 235 °C, (c) 250 °C and (d) 255 °C, respectively. The features marked by the asterisk are originated from the sapphire substrate.

Table 1
Electrical properties of the ZnO:N samples grown on (a) a-Al_2O_3 and (b) c-Al_2O_3 at various T_{Zn}.

	Resistivity (ohm.cm)	Hall mobility (cm^2/V s)	Carrier concentration (cm^{-3})	Carrier type
a				
235	0.14	12.68	3.58×10^{18}	n
240	3.97	0.24	6.68×10^{18}	n
245	0.03	16.62	1.13×10^{19}	n
250	128	0.25	2.30×10^{17}	n
255	2.60×10^4	0.35	9.53×10^{14}	n
b				
235	3.41	0.52	3.46×10^{18}	n
240	2.64	0.85	2.60×10^{18}	n
245	7.05	0.12	2.60×10^{18}	n
250	38.71	1.20	2.60×10^{17}	n
255	202.14	1.33	2.60×10^{16}	p

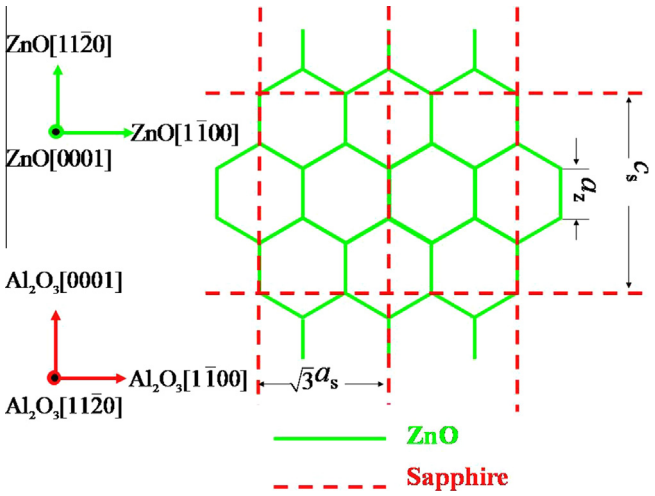

Fig. 2. Schematic diagram showing the epitaxial relationships of the ZnO (0001) grown on Al_2O_3 (11$\bar{2}$0). (a_s and c_s denoted as the a- and c-axis lattice parameters of Al_2O_3, respectively. a_z denoted as the a-axis lattice parameters of ZnO.)

about −18.4% considering 30° in-plane rotation in the relationship of ZnO[2$\bar{1}\bar{1}$0]||Al_2O_3[1$\bar{1}$00] and ZnO[1$\bar{1}$00]||Al_2O_3[1$\bar{2}$10] [20]. Fig. 2 shows the schematic diagram of the epitaxial relationships between ZnO and a-Al_2O_3. In Fig. 2, the dot lines represent the atom arrangement in a-plane Al_2O_3 and the solid lines represent the atom arrangement in c-plane ZnO. a_s and c_s denoted as the a- and c-axis lattice parameters of Al_2O_3, respectively. a_z denoted as the a-axis lattice parameter of ZnO. From Fig. 2, it can be found that the lattice parameter along the Al_2O_3[0001], 12.991 Å, is almost equal to the four times of the lattice parameter along ZnO[11$\bar{2}$0], 12.996 Å. And two times of the lattice parameter along Al_2O_3[1$\bar{1}$00], 16.486 Å, is almost equal to the three times of the lattice parameter along ZnO[1$\bar{1}$00], 16.574 Å. From above analysis, the mismatch between a-Al_2O_3 and ZnO is only −0.038% with the relationship of ZnO[11$\bar{2}$0]||Al_2O_3[0001] and −2.4% with the relationship of ZnO[1$\bar{1}$00]||Al_2O_3[1$\bar{1}$00], respectively. The "–" denotes that the lattice parameter of substrate is smaller than that of epitaxial layer, meaning in-plane compressive stress in the ZnO films. According to the above results, it can be found that the compressive stress in the ZnO:N⟨c⟩ films should be larger than that of in the ZnO:N⟨a⟩ films. Generally, this compressive stress in films raises the formation energy of N_O, because the radius of N^{3-} (1.71 Å) is larger than that of O^{2-} (1.32 Å). However, the compressive stress can be relaxed after depositing few atom layers due to the large lattice mismatch. Thus, the No defect can form more easily than the case on a-plane sapphire. Therefore, the ZnO:N⟨c⟩ films are lower in the carrier concentration and stronger in the intensity of the Raman peaks located at 275 cm^{-1}, which were consistent with Raman and Hall-effect measurements.

80 K-PL spectra of ZnO:N⟨a⟩ and ZnO:N⟨c⟩ films grown at the T_{Zn} of 235, 250 and 255 °C were shown in Fig. 3a, b and c, respectively. From Fig. 3a and b, it can be found that each PL spectrum is dominated by a neutral donor-bound exciton (D°X) at 3.368 eV due to formation of donor-like defects and a donor-acceptor pair (DAP) emission peak located around 3.253 eV for N-doping [21]. Two other weak peaks in PL spectrum are at 3.181 and 3.109 eV, which are 72 and 144 meV away from DAP emission, respectively. Therefore, these two peaks can be attributed to the 1 and 2-LO phonon mediated recombination of the DAP. The peak at 3.333 eV in PL spectrum marked by asterisk in the Fig. 3a, b and c was attributed to the excitions bound to structural defects [22]. From Fig. 3c, except DAP emission peak, a weak UV emission peak located at 3.356 eV was also observed, which is attributed to the emission of excitons bound to neutral acceptors (A°X) induced by N doping

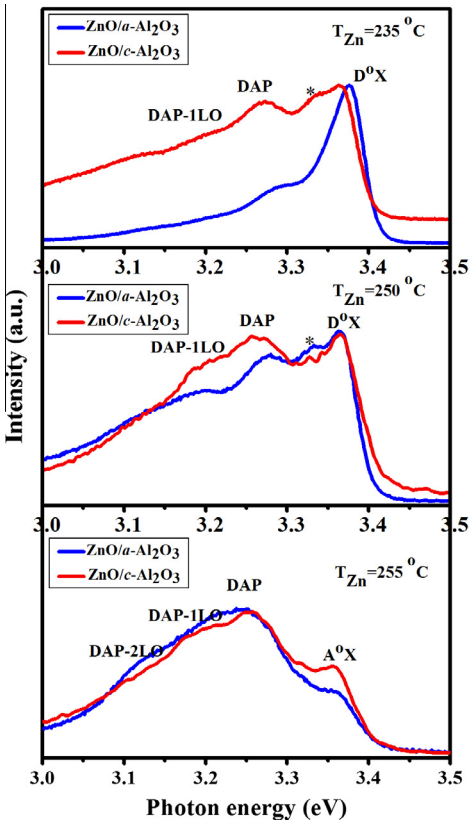

Fig. 3. 80 K-PL spectra of ZnO:N films grown on a-/c-Al_2O_3 at the T_{Zn} of (a) 235, (b) 250 and (c) 255 °C.

[23]. For the ZnO:N films grown at the T_{Zn} of 235 and 250 °C, the D°X located around 3.368 eV is dominant in all spectra regardless of substrate and T_{Zn}. However, for the film grown at the T_{Zn} of 255 °C, the DAP emission band located at 3.253 eV is dominant in the PL spectrum as shown in Fig. 3c. As above discussion, the intensity ratio of the DAP/D°X emission increases with increasing T_{Zn}, which implied that the N acceptor content was enhanced by increasing T_{Zn}. Compared with the ZnO:N⟨*a*⟩ films, the intensity ratio of the DAP/D°X emission is larger for the ZnO:N⟨*c*⟩ films grown at the same T_{Zn}, which means N has a higher incorporation efficiency in ZnO:N⟨*c*⟩ films.

4. Conclusion

The doping efficiency of nitrogen in ZnO films grown on *a*-/*c*-Al_2O_3 were investigated. It was shown that enhancement of the incorporation efficiency of N can be achieved by using *c*-Al_2O_3 substrates, as determined by the Raman and XPS measurement. This was attributed to the better relaxation of compressive stress induced by lattice mismatch in the ZnO films grown on *c*-Al_2O_3 is larger than that of the films grown on *a*-Al_2O_3. It benefits for the incorporation efficiency of N in ZnO films.

Acknowledgements

This work is supported by the National Basic Research Program of China (973 Program No. 2011CB302005), the National Natural Science Foundation of China (Nos. 11074248, 10874278, 60806002 and 10974197), the 100 Talents Program of the Chinese Academy of Sciences, and the Ph.D. Science Research Foundation of Yancheng Teachers University (No. 12YSYJB0111).

References

[1] D.C. Look, Mater. Sci. Eng. B 80 (2001) 383.
[2] Z.K. Tang, G.K.L. Wong, P. Yu, Appl. Phys. Lett. 72 (1998) 3270.
[3] Y. Zhu, S.S. Lin, Y.Z. Zhang, Z.Z. Ye, Y.F. Lu, J.G. Lu, B.H. Zhao, Appl. Surf. Sci. 255 (2009) 6201.
[4] M.A. Myers, M.T. Myers, M.J. General, J.H. Lee, L. Shao, H. Wang, Appl. Phys. Lett. 101 (2012) 112101.
[5] N.T. Huong, N.V. Tuyen, N.H. Hong, Mater. Chem. Phys. 126 (2011) 54.
[6] K.C. Chiu, Y.H. Wu, Adv. Mater. Res. 415 (2011) 1925.
[7] Q.P. Wang, Z. Sun, J. Du, P. Zhao, X.H. Wu, X.J. Zhang, Opt. Mater. 29 (2007) 1358.
[8] H.J. Jin, B. Xu, C.B. Park, Trans. Electr. Electron. Mater. 12 (2011) 169.
[9] B.Y. Zhang, B. Yao, Y.F. Li, Z.Z. Zhang, B.H. Li, C.X. Shan, D.X. Zhao, D.Z. Shen, Appl. Phys. Lett. 97 (2010) 222101.
[10] S. Shet, K.S. Ahn, R. Nuggehalli, Y.F. Yan, J. Turner, M.A. Jassim, Thin Solid Films 519 (2011) 5983.
[11] L.L. Chen, J.G. Lu, Z.Z. Ye, Y.M. Lin, B.H. Zhao, Y.M. Ye, J.S. Li, L.P. Zhu, Appl. Phys. Lett. 87 (2005) 252106.
[12] C. Li, M. Furuta, T. Matsuda, T. Hiramatsu, H. Furuta, T. Hira, Thin Solid Films (2009) 3265.
[13] J.L. Zhao, X.M. Lia, J.M. Biana, W.D. Yu, C.Y. Zhang, J. Cryst. Growth 280 (2005) 495.
[14] S. Yamauchi, Y. Goto, T. Hariu, J. Cryst. Growth 260 (2004) 1.
[15] K. Tamura, T. Makino, A. Tsukazaki, M. Sumiy, S. Fuke, T. Furumochi, M. Lippmaa, C.H. Chia, Y. Segawa, H. Koinuma, M. Kawasaki, Solid State Commun. 127 (2003) 265.
[16] B.T. Adekore, J.M. Pierce, R.F. Davis, D.W. Barlage, J.F. Muth, J. Appl. Phys. 102 (2007) 024908.
[17] .C. Klingshirn, Phys. Stat. Sol. B 244 (2007) 302.
[18] A. Kaschner, U. Haboeck, Martin Strassburg, Matthias Strassburg, G. Kaczmarczyk, A. Hoffmann, C. Thomsen, A. Zeuner, H.R. Alves, D.M. Hofmann, B.K. Meyer, Appl. Phys. Lett. 80 (2002) 1909.
[19] X.Y. Duan, R.H. Yao, Y.J. Zhao, Appl. Phys. A 91 (2008) 467.
[20] Ü. Özgür, Ya.I. Alivov, C. Liu, A. Teke, M.A. Reshchikov, S. Doğan, V. Avrutin, S.-J. Cho, H. Morkoç, J. Appl. Phys. 98 (2005) 041301.
[21] D.C. Look, D.C. Reynolds, C.W. Litton, R.L. Jones, D.B. Eason, G. Cantwell, Appl. Phys. Lett. 81 (2002) 1830.
[22] B.K. Meyer, H. Alves, D.M. Hoffman, W. Kriegseis, D. Forster, F. Bertram, J. Christen, A. Hoffman, M. Strassburg, M. Dworzak, U. Haboeck, A.V. Rodina, Phys. Status Solidi B 241 (2004) 231.
[23] A. Teke, Ü. Özgür, S. Doğan, X. Gu, H. Morkoç, B. Nemeth, J. Nause, H.O. Everitt, Phys. Rev. B 70 (2004) 195207.